New Journal of Chemistry - Electronic Supplementary Information

Aqueous dispersions of highly luminescent boron-rich nanosheets by the exfoliation of polycrystalline titanium diboride

Saju K. John and Aji A. Anappara

Department of Physics, Photonic Materials and Devices Laboratory, National Institute of Technology Calicut (NITC), Kozhikode-673601, Kerala, India

I. Crystal structure of TiB_2, digital images of pristine TiB_2 and boron-rich nanosheets in powder form

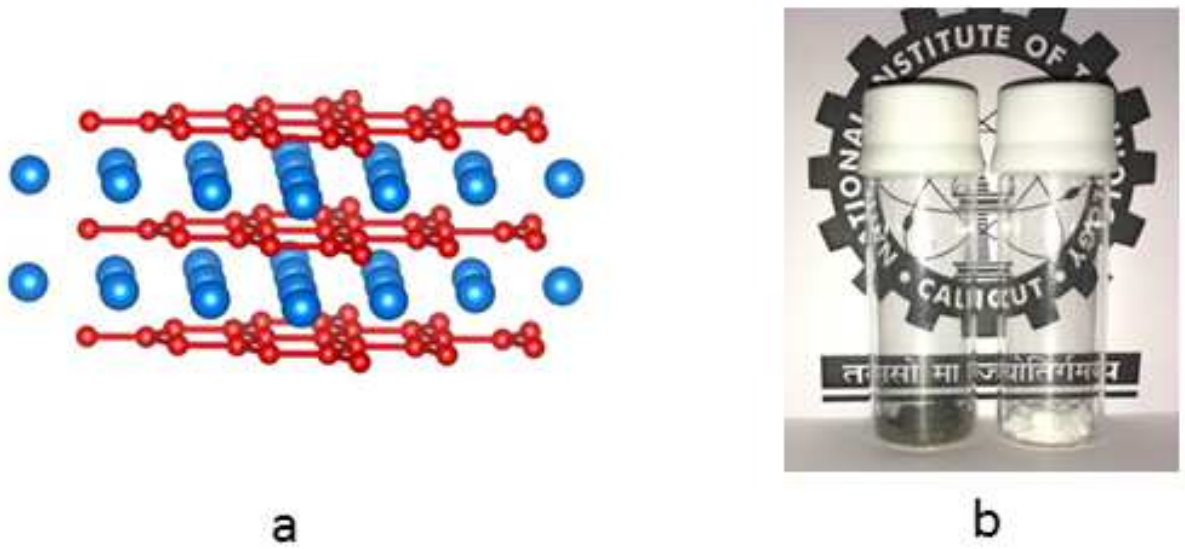

Fig. S0: (a) Schematic representation of the crystal structure of the TiB_2. Ti atoms are indicated by blue balls and the B atoms as red balls. The boron atoms form a hexagonal network similar to carbon network in graphene. (b) Digital photographs of pristine TiB_2 powder (right) and the boron-rich nanosheets in powder form, obtained through lyophilization of the aqueous dispersion.

II. Field Emission Scanning Electron Microscopy (FESEM) images of pristine TiB_2

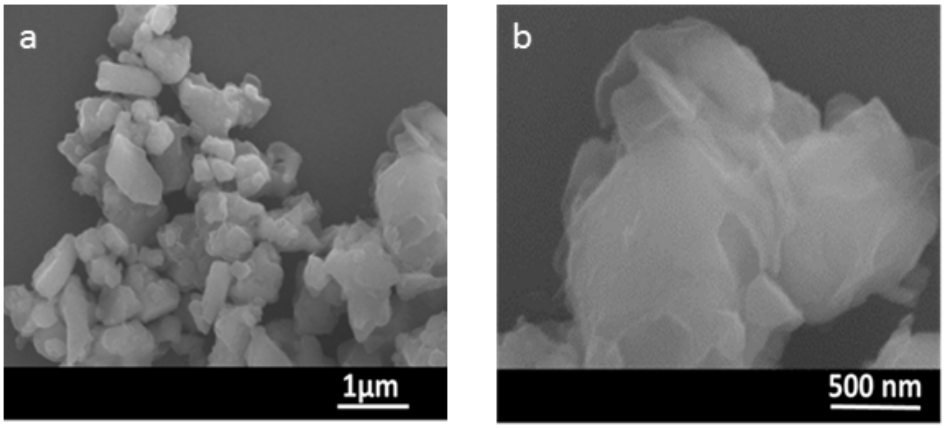

Fig. S1: (a) & (b) FESEM images of bulk TiB_2 powder. The magnified SEM image (in the right panel) shows a layered appearance of bulk TiB_2 particles.

III. X-ray Diffraction Analysis (XRD) of bulk TiB_2 powder

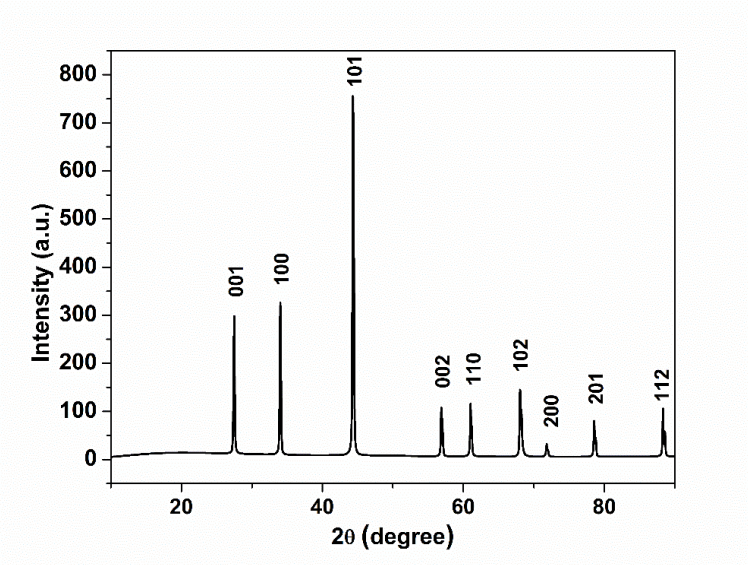

Fig. S2: X-ray diffraction (XRD) pattern of pristine TiB_2 powder sample.

The X-ray diffraction (XRD) data of the bulk TiB_2 powder sample was obtained in RigakuMiniflex 300 X-ray Diffractometer. The positions of X-ray peaks (2Θ values) and the error (estimated standard deviation, ESD) in each 2Θ value as measured by the instrument are included in table S1 (columns 2 and 3 respectively).

The calculation of the unit cell parameters along with the possible errors is discussed below.

Calculation of lattice parameters from X-ray diffraction (XRD) data

Columns 4 and 5 of table S1 respectively are the d-spacings and the corresponding ESDs calculated by the instrument from Bragg's equation. Lattice parameters (a and c of hcp unit cell of TiB_2) were calculated from d-spacings, using the equation $\frac{1}{d^2}=\left[\frac{4}{3}\left(h^2+k^2+hk\right)+l^2\left(\frac{a}{c}\right)^2\right]\frac{1}{a^2}$, connecting the inter-planar spacing (d), Miller indices (h, k, l) and lattice parameters (a and c) for a hexagonal lattice. The Miller indices (column-6 of table S1) corresponding to various 2Θ values were adopted from reference R1. The calculated values of lattice parameters (a and c) along with the errors are included in the last four columns of table S1.

Table S1: Calculation of lattice parameters from XRD data of the pristine TiB_2 powder sample.

Sl. No.	2Θ(deg)	ESD in 2Θ(deg)	d (Å)	ESD in d (Å)	h k l	a (Å)	Error in a(Å)	c (Å)	Error in c (Å)
1	27.4893	0.009672	3.24206	0.001118	001			3.2421	0.0011
2	32.0267	0.011956	2.63264	0.000897	100	3.0399	0.0042		
3	44.3418	0.004963	2.04122	0.000217	101	3.0339	0.0031	3.2323	0.0007
4	56.8582	0.014357	1.61803	0.000374	002			3.2361	0.0004
5	61.0203	0.012442	1.51725	0.000279	110	3.0345	0.0003		
6	68.0431	0.008047	1.37675	0.000143	102	3.0259	0.0002	3.2326	0.0002
7	71.8182	0.012591	1.31338	0.000199	200	3.0331	0.0002		
8	78.5489	0.00818	1.21683	0.000106	201			3.2285	0.0001
9	88.3188	0.01326	1.1057	0.000132	112	3.0306	0.0002	3.2312	0.0002

The average values of a and c respectively were calculated as 3.033 ± 0.0014 Å and 3.234 ± 0.0004 Å. The unit cell parameters obtained are close to the typical (JCPDS data) values for lattice parameters of TiB_2: a = 3.029Å, c = 3.228 Å.[R2]

IV. UV-visible absorption spectrum (UV-DRS) of pristine TiB_2 in powder form

The diffuse reflectance spectrum (DRS) of solid samples (as included in Fig. S3) was collected using a spectrometer (PerkinElmer, Model: LAMBDA 650) equipped with an integrating sphere. Barium sulphate ($BaSO_4$) was used as the reference material. The absorption $\left({}^{\alpha}/_{S}\right)$ data were calculated from the reflectance spectra using the Kubelka–Munk function: ${}^{\alpha}/_{S} = \frac{(1-R)^2}{2R}$; where R is the reflectance at a given wavelength, and α is the absorption coefficient, and S is the scattering coefficient (practically wavelength-independent when the flake size is much larger than wavelength of light).

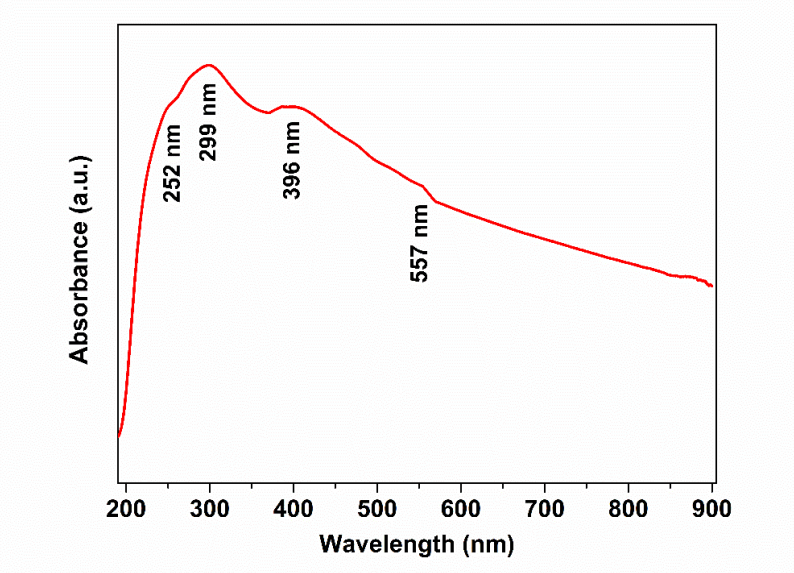

Fig. S3: The absorption spectrum of bulk TiB_2 powder samples collected at room temperature by UV-vis diffuse reflectance spectroscopy (DRS).

V. Photoluminescence spectra of bulk TiB_2 powder

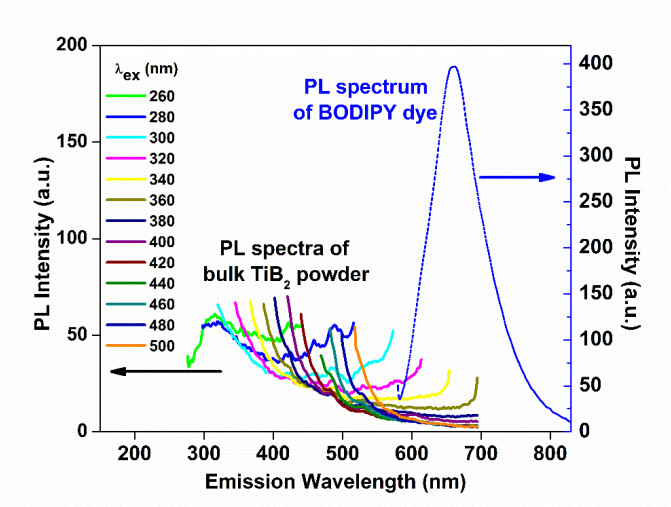

Fig. S4: Photoluminescence (PL) spectra of the pristine TiB_2 powder sample collected at different excitation wavelengths from 260 to 500 nm. PL spectrum of BODIPY dye in powder form, excited at λ = 560 nm, is also reported by the dashed curve to give an idea of the magnitude of emission.

The photoluminescence (PL) spectra of the bulk TiB_2 powder sample collected at different excitation wavelengths from 260 to 450 nm (as illustrated in Fig. S4). The figure shows that the photoluminescence of the bulk TiB_2 powder is extremely weak compared to the background noise. In order to get an idea of the magnitude of emission, since the spectrofluorometer gives intensity in arbitrary unit, PL data for BODIPY dye (boron-dipyrromethene; 4,4-difluoro-4-bora-3a,4a-diaza-s-indacene) in the powder form was also collected at identical conditions, and is plotted along with the data obtained for TiB_2 powder. The BODIPY dyes are known for their photoluminescence in the solid-state. The PL quantum yield of BODIPY in the solid state is ~ 10 %, meanwhile when dissolved in water is ~70%.[R3] Also, the steady-state, absolute PL quantum yield (QY) of TiB_2 powder sample was obtained using an integrating sphere set up in a FluoroLog-322 (Horiba equipped with a 450 W Xe arc lamp) to collect the emitted light in all solid angles. The measurement was done by using barium sulphate ($BaSO_4$) as the matrix to incorporate TiB_2 powder. The photoluminescence QY of the TiB_2 powder (with respect to the matrix standard) was found to be as small as 0.3 %. This extremely small absolute QY confirms the poor photoluminescence of the bulk TiB_2 powder sample.

VI. Transmission electron microscopy (TEM) images and SAED patterns of boron-rich nanosheets

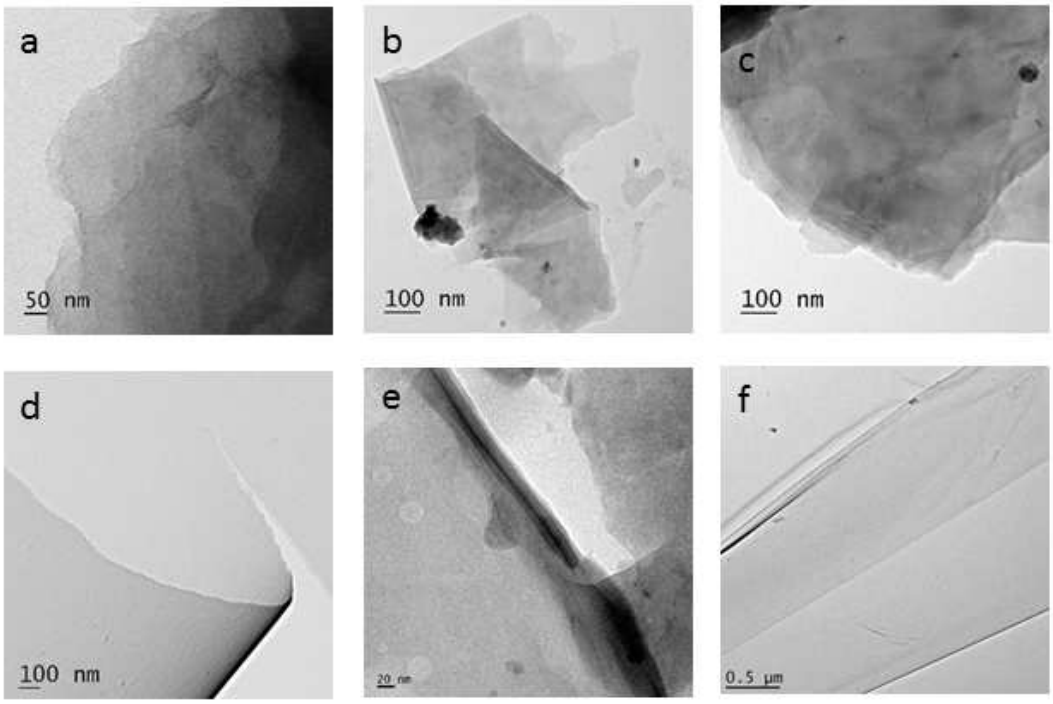

Fig. S5: TEM images of the nanosheets obtained by depositing the dialyzed dispersion on the TEM grid.

TEM analysis was performed by depositing the nanosheet dispersion on the holey carbon coated TEM grid. All the nanostructures appeared to be having sheet like structure and most of them with a quasi-planar morphology (Fig S5. a,c, and f). Some of the nanosheets are found to have folds as shown in Fig. S5 b, d and e, while some other nanosheets possessed tearing on them (Fig. S5 d and e). Overlapping of nanosheets was observed for some nanosheets as in Fig S5 a and c.

The SAED patterns obtained under TEM from various regions of several boron-rich nanosheets are given in Fig. S6. The diameters (2D) of various rings in the SAED patterns were measured using image-J software. The reciprocals of these D values are calculated, which gives the d-spacings. Those d-spacings calculated from the various SAED patterns of boron-rich nanosheets are given in table S2.

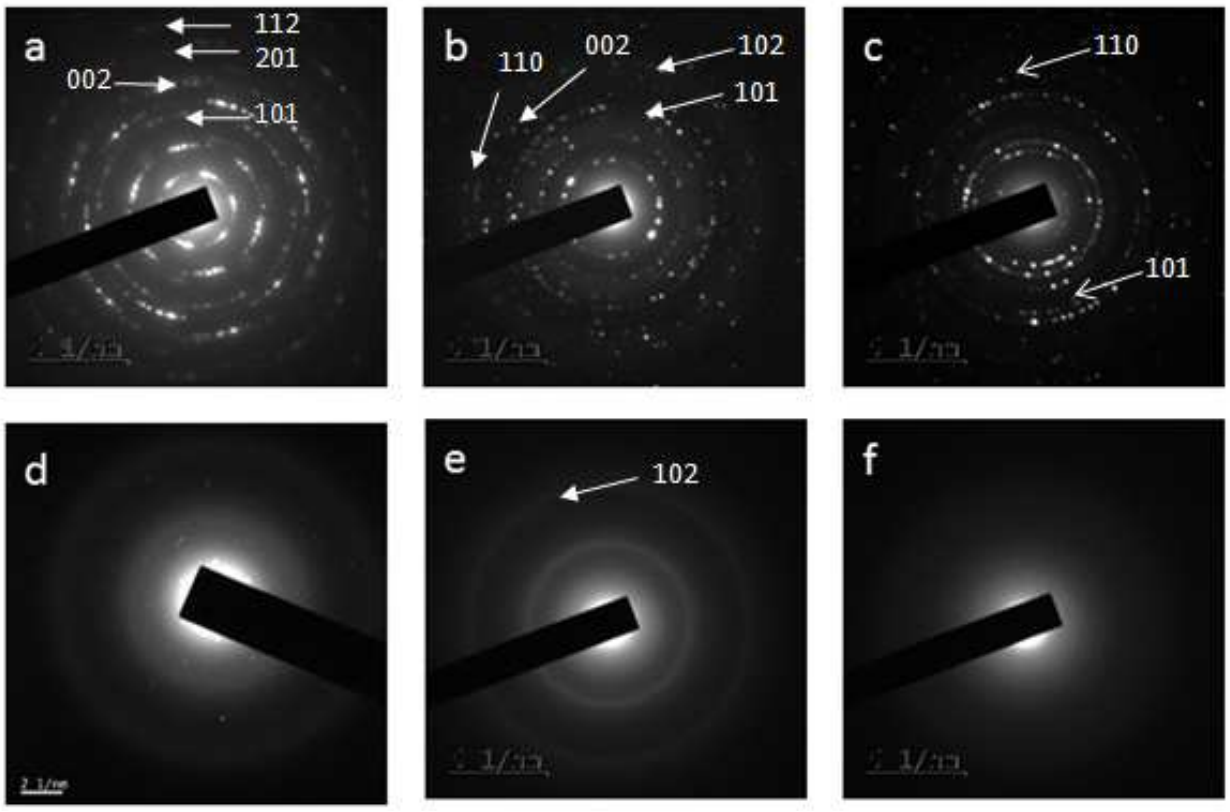

Fig. S6: SAED patterns obtained on various regions of several boron-rich nanosheets. a-d shows the polycrystalline nature and e & f, amorphous nature of boron rich nanosheets. The hkl values were assigned after calculating the d-spacings (table S2) and matching those values with XRD data.

Table S2: Calculation of d-spacings from SAED patterns of boron-rich nanosheets. The hkl values (given in brackets) were assigned after matching the d-values with XRD data (table S1).

Fig. S6 (a)		**Fig. S6 (b)**		**Fig. S6 (c)**		**Fig. S6 (d)**		**Fig. S6 (e)**	
2D (nm^{-1})	**d=1/D (Å)**	**2D (nm^{-1})**	**d=1/D (Å)**	**2D (nm^{-1})**	**d=1/D (Å)**	**2D (nm^{-1})**	**d=1/D (Å)**	**2D (nm^{-1})**	**d=1/D (Å)**
19.0355	1.0507 (112)	4.8926	4.0878	13.3968	1.4929 (110)	11.2102	1.7841	8.018	2.4944
16.8524	1.1868 (201)	7.2642	2.7532	11.5234	1.7356	6.5517	3.0527	13.878	1.4411 (102)
12.6445	1.5817 (002)	9.1182	2.1934	10.6228	1.8827				
10.9534	1.8259	10.1913	1.9624 (101)	10.0345	1.9931 (101)				
9.6886	2.0643 (101)	11.5930	1.7252	8.1947	2.4406				
7.3252	2.7303	12.6095	1.5861 (002)	6.7850	2.9477				
6.4633	3.2317	13.0767	1.5294 (110)	5.7433	3.4823				
3.6992	5.4065	14.649	1.3653 (102)	3.5102	5.6976				

Some of the d-spacings in table S2, as estimated from the SAED data, were found to be matching with d-spacings obtained from the XRD data of bulk TiB_2; as given in Table S1. Some other d-spacings in table S1 were found not to be matching with d-spacings obtained from the XRD data bulk TiB_2. This may be due to two reasons (i) in the SAED pattern, since the zone axis is not aligned in the plane, some out of plane reflections can be present and (ii) as we have discussed in the article, the nanosheets are chemically modified (containing –OH functional groups and having titanium deficient stoichiometry) and therefore, may not have perfect TiB_2 crystalline structure.

For convenience of the readers, table S1 is copied below.

Table S1: Calculation of lattice parameters from XRD data of the bulk TiB_2 powder sample.

Sl. No.	2Θ(deg)	ESD in 2Θ(deg)	d (Å)	ESD in d (Å)	h k l	a (Å)	Error in a(Å)	c (Å)	Error in c (Å)
1	27.4893	0.009672	3.24206	0.001118	001			3.2421	0.0011
2	32.0267	0.011956	2.63264	0.000897	100	3.0399	0.0042		
3	44.3418	0.004963	2.04122	0.000217	101	3.0339	0.0031	3.2323	0.0007
4	56.8582	0.014357	1.61803	0.000374	002			3.2361	0.0004
5	61.0203	0.012442	1.51725	0.000279	110	3.0345	0.0003		
6	68.0431	0.008047	1.37675	0.000143	102	3.0259	0.0002	3.2326	0.0002
7	71.8182	0.012591	1.31338	0.000199	200	3.0331	0.0002		
8	78.5489	0.00818	1.21683	0.000106	201			3.2285	0.0001
9	88.3188	0.01326	1.1057	0.000132	112	3.0306	0.0002	3.2312	0.0002

XRD-data of boron-rich nanosheets was also collected and is displayed in Fig. S7. Powder obtained by the lyophilisation of boron-rich nanosheet dispersion was used for the XRD data collection. Fig. S7 presents an amorphous nature of boron-rich nanosheets except for a crystalline peak observed at 28.044^0. This peak corresponds to the (001) plane (see table S1) of bulk TiB_2.

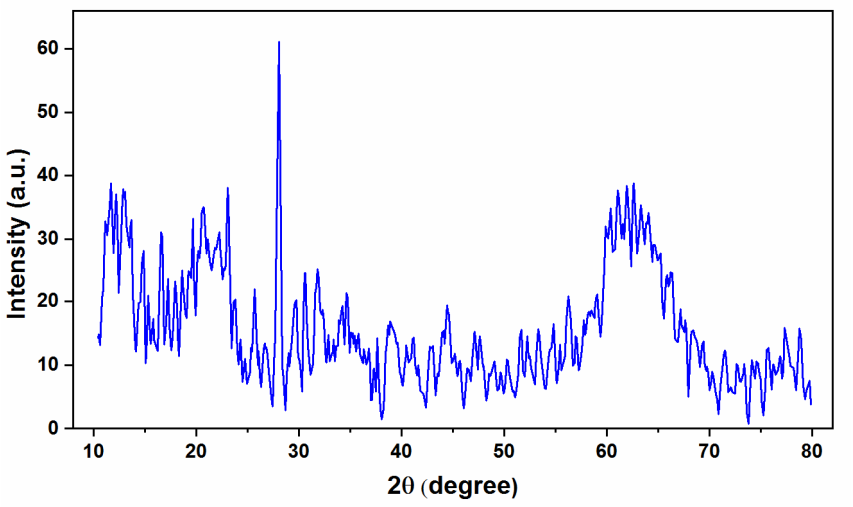

Fig. S7: XRD pattern of boron-rich nanosheet powder sample.

VII. Determination of stoichiometric ratio of Ti and B in the nanosheets using Inductively coupled plasma atomic emission spectroscopy (ICP-AES)

The concentrations of Ti and B (mg/L) in the dialyzed dispersion of nanosheets were obtained by ICP-AES analysis. The Ti:B stoichiometric ratio is calculated as:

$$\frac{Elemental concentration of Ti}{Atomic weight of Ti (47.87)} : \frac{Elemental concentration of B}{Atomic weight of B (10.81)}$$

The table displays much lesser Ti : B ratio in nanosheets as compared to the 1:2 ratio in pristine TiB_2.

Table S3: ICP-AES analysis results of boron rich nanosheet dispersion

Sample	**Concentration measured by ICP-AES (mg/L)**		**Stoichiometric ratio**
	Ti	B	Ti : B
1	0.164	0.106	0.29 : 2
2	7.442	0.999	0.06 : 2

VIII. Luminescence spectra of boron-rich nanosheets in aqueous dispersion

The fluorescence excitation spectrum (blue curve) of the aqueous dispersion of boron-rich nanosheets, collected by fixing the emission wavelength at 445 nm is displayed in Fig. S8 (a). The spectrum possesses strong peaks at 220 nm and 350 nm and a shoulder peak at 234 nm. These peaks are close to the corresponding shoulders (at 227 nm, 250 nm and 355 nm) in the UV-Vis absorption spectrum of the dispersed nanosheets (as shown in Fig. 3 of the main article). The excitation spectrum shows the highest intensity at 350 nm. The emission spectrum obtained at an excitation wavelength of 350 nm is also depicted (red curve in Fig. S8).

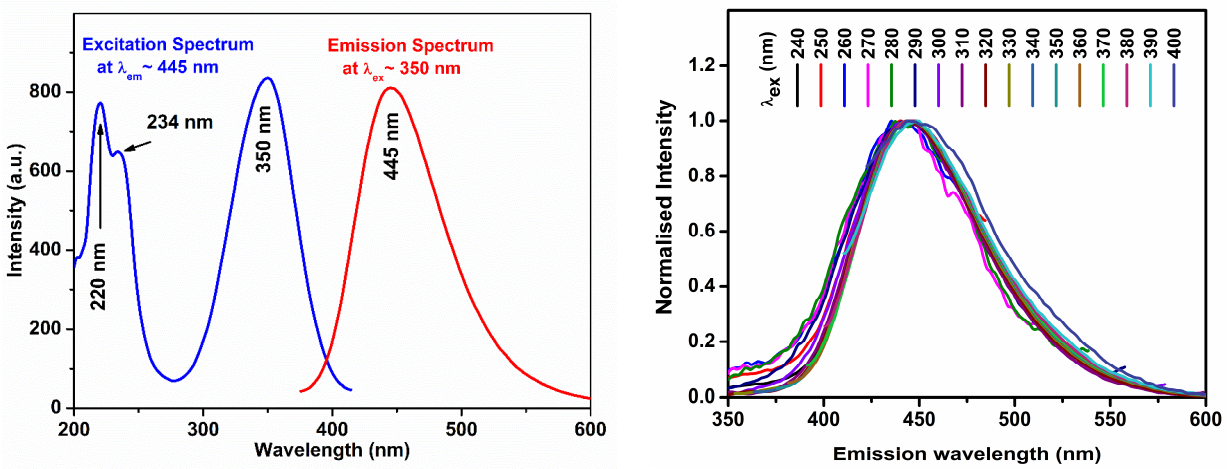

Fig. S8 (a) Photoluminescence (PL) emission spectrum (red curve) of the TiB_2 nanosheet dispersion obtained for an excitation of 350 nm along with the corresponding excitation spectrum (blue curve). (b) Intensity normalized PL spectra showing the excitation independent nature of nanosheets.

IX. Photoluminescence Quantum Yield (QY) calculation

The relative quantum yield of TiB_2 nanosheet dispersion was calculated taking Quinine sulfate as a reference using the following equation.

$$QY = QY_{ref}\left(\frac{n}{n_{ref}}\right)^2 \frac{I}{I_{ref}}\frac{A_{ref}}{A}$$

QY_{ref} , n_{ref} , I_{ref} and A_{ref} are respectively the quantum yield, refractive index, integrated fluorescence intensity and absorbance at the excitation wavelength of the reference compound (Quinine sulfate) and QY, n, I and A are respectively those the aqueous dispersion of nanosheets. The quantum yield of the reference compound (Quinine sulfate), QY_{ref} ~ 0.54 and the ratio ofthe refractive indices was approximated as 1, in the calculation.

The Quantum Yield (QY) of the TiB_2 nanosheet dispersion is thus obtained as,

$$\text{QY} = 0.54 \times 1 \times \frac{25907.08}{67814.28} \times \frac{0.017}{0.026} = 0.13 = 13\%$$

X. TEM images of boron-rich nanosheets (after aging for 2 months)

Transmission electron microscopy was employed in order to investigate the stability of the nanosheets upon aging. For this purpose, we have collected the TEM image of nanosheets samples two months after the synthesis. The synthesis procedure of the nanosheets is identical to that explained in the manuscript. The samples for TEM analysis was prepared by depositing the aqueous dispersion of nanosheets on to a holey copper grid supported with a carbon film. The optical properties of the nanosheets (UV-vis absorption spectrum as well as PL spectra) were intact in the repetition of the experiments even 6 months after the synthesis was performed. The aqueous dispersion was found to be stable without any flocculation or sedimentation; also, the pH of the solution remained constant without any noticeable change for tenure of 6 months. The reasons behind the crumbling effect of the nanosheets (observed under TEM) by aging, may warrant detailed investigation; hence it is beyond the scope of this article.

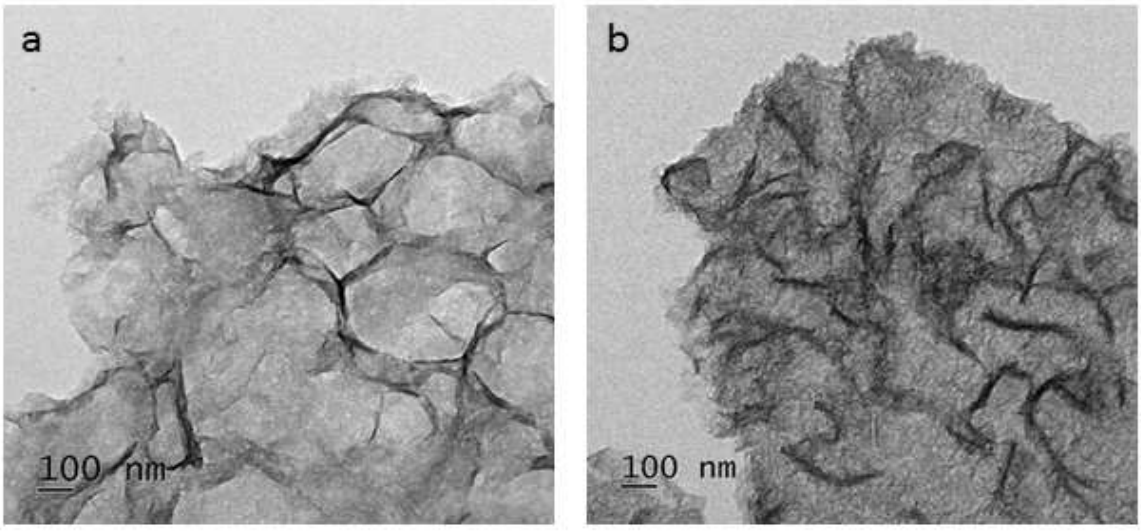

Fig. S9: Transmission electron microscopy (TEM) images collected after 2 months of synthesis.

XI. X-ray Diffraction (XRD) analysis of boron-rich nanosheet powder

The percentage of crystallinity of boron-rich nanosheet powder sample was estimated by analyzing the X-ray diffraction pattern of the sample.

The X-ray diffraction pattern of TiB_2 nanosheet powder samples (Fig. S10) presents an amorphous nature of TiB_2 nanosheets, except for the presence of a crystalline peak observed at 28.044°. This peak at 28.044° is corresponding to the (001) plane of bulk TiB_2 (see table S1). The percentage of crystallinity of the nanosheet sample was calculated by analyzing the area under the curve using origin pro software and it was found that the sample is 2.8% crystalline and 97.2% amorphous. The calculation is explained below.

The percentage of crystallinity was calculated by using the equation,

$$Crystallinity = \left\{\frac{Area\ of\ crystalline\ peaks}{Area\ of\ all\ peaks\ (crystalline + amorphous)} \times 100\right\} = \frac{28.20702}{100.175}$$

$$= 2.8\%$$

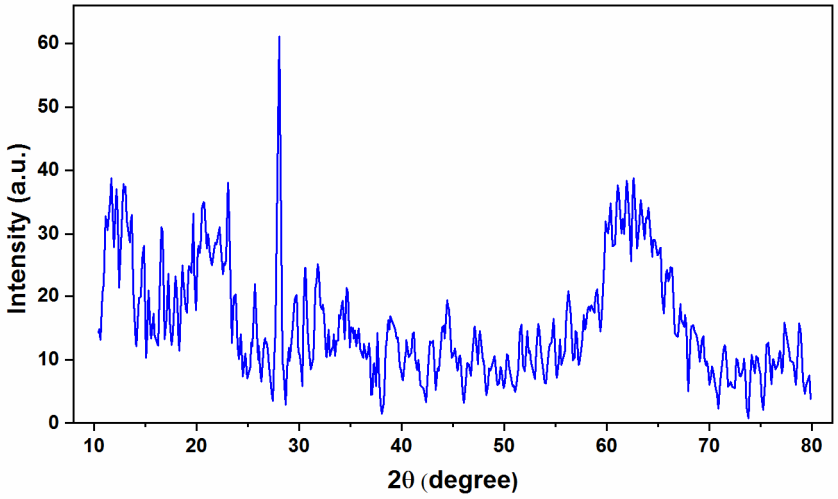

Fig. S10: X-ray diffraction (XRD) pattern of pristine TiB_2 nanosheet powder sample

REFERENCES:

R1 M. Ipekci, S. Acar, M. Elmadagli, J. Hennicke, O. Balci, and M. Somer, *Ceramics International*, 2017, **43**, 2039-45.

R2 S. Chakraborty, D. Debnath, A. R. Mallick, and P. K. Das, Int. Journal of Refractory Metals and Hard Materials,2014, **46**, 35-42.

R3 S. Xiao, Q. Cao, and F. Dan, Curr. Org. Chem., 2012, **16**, 2970-81.

R4 D. B. Williams and C. B. Carter, Transmission Electron Microscopy: A Text Book for Material Science, Springer US, 2009.